



This is the accepted manuscript made available via CHORUS. The article has been published as:

Contribution of nuclear excitation electromagnetic form factors in math

C ¹² and O ¹⁶ to the Coulomb sum rule

A. Bodek and M. E. Christy

Phys. Rev. C **107**, 054309 — Published 19 May 2023

DOI: [10.1103/PhysRevC.107.054309](https://doi.org/10.1103/PhysRevC.107.054309)

Contribution of Nuclear Excitation Electromagnetic Form Factors in ^{12}C and ^{16}O to the Coulomb Sum Rule

A. Bodek¹ and M. E. Christy²

¹*Department of Physics and Astronomy, University of Rochester, Rochester, NY 14627, USA*

²*Thomas Jefferson National Accelerator Facility, Newport News, VA 23606, USA*

(Dated: April 14, 2023)

We report on empirical parameterizations of longitudinal and transverse nuclear excitation electromagnetic form factors in ^{12}C and ^{16}O . We extract the contribution of nuclear excitations to the Normalized Inelastic Coulomb Sum Rule ($S_L(\mathbf{q})$) as a function of momentum transfer \mathbf{q} and find that it is significant (0.29 ± 0.030 at $\mathbf{q} = 0.22$ GeV). The total contributions of nuclear excitations to $S_L(\mathbf{q})$ in ^{12}C and ^{16}O are found to be equal within uncertainties. Since the cross sections for nuclear excitations are significant, the radiative tails from nuclear excitations should be included in precise calculations of radiative corrections to quasielastic electron scattering at low \mathbf{q} and deep-inelastic electron scattering at large energy transfers ν . The parameterizations also serve as a benchmark in testing theoretical modeling of cross sections for excitation of nuclear states in electron and neutrino interactions on nuclear targets at low energies.

I. INTRODUCTION

The Normalized Inelastic Coulomb Sum Rule $S_L(\mathbf{q})$ [1] in electron scattering on nuclear targets is the integral of the longitudinal nuclear response function $R_L(\mathbf{q}, \nu) d\nu$ (excluding the nuclear elastic peak and pion production processes) divided by the square of the proton electric form factor and by the number of protons in the nucleus. Here, \mathbf{q} is the momentum transfer and ν is the energy transfer to the nuclear target. The sum rule has contributions from quasielastic (QE) scattering and from the electro-excitations of nuclear states. At high \mathbf{q} it is expected that $S_L \rightarrow 1$ because both nuclear excitation form factors and Pauli suppression are small. At small \mathbf{q} it is expected that $S_L \rightarrow 0$ because all cross sections for inelastic processes (e.g. QE, nuclear excitation and pion production processes) must be zero at $\mathbf{q}=0$.

In this paper we present details of empirical parameterizations of the \mathbf{q} dependence of all longitudinal and transverse excitation form factors in ^{12}C . Since there are fewer measurements on ^{16}O we only parameterize the longitudinal form factors for this nucleus. We use these parameterizations to compute the contribution of nuclear excitations to $S_L(\mathbf{q})$ for both nuclei. Our investigation of the QE contribution to $S_L(\mathbf{q})$ is reported in an earlier publication[2].

Since the cross sections for nuclear excitations are significant at low \mathbf{q} , the parametrizations should be used in precise calculations of radiative corrections to quasielastic electron scattering at low \mathbf{q} . Because of initial state radiation, nuclear excitations also contribute to radiative corrections in deep-inelastic electron scattering at large ν .

The parameterizations also serve as benchmark in testing theoretical modeling of electron and neutrino scattering at low energies. Because of recent advances in theoretical methods[3–5] for the calculations of the response functions of electron scattering on nuclear targets, it is now possible to make theoretical predictions of the form

factors for the excitation of nuclear states in both electron and neutrino scattering[6–8].

Figures 1 and 2 show the relative contributions of the cross sections for elastic scattering from the ^{12}C nucleus compared to the first three low lying excitations of nuclear states for several incident energies and scattering angles [9–11]. Also shown as a solid curve is our parameterization where we have used the experimental resolution to apply a Gaussian smearing to each state.

II. THEORETICAL FRAMEWORK

The electron scattering differential cross section can be written in terms of longitudinal ($R_L(\mathbf{q}, \nu)$) and transverse ($R_T(\mathbf{q}, \nu)$) nuclear response functions [12]:

$$\frac{d\sigma}{d\nu d\Omega} = \sigma_M [A R_L(\mathbf{q}, \nu) + B R_T(\mathbf{q}, \nu)] \quad (1)$$

where σ_M is the Mott cross section,

$$\sigma_M = \frac{\alpha^2 (\cos^2(\theta/2))}{4E_0^2 \sin^4(\theta/2)}. \quad (2)$$

Here, $\alpha_F = 1/137$ is the fine structure constant, E_0 is the incident electron energy, E' is energy of the final state electron, $\nu = E_0 - E'$ is the energy transfer to the target, \mathbf{q} is the 3-momentum transfer, Q^2 is the square of the 4-momentum transfer (defined to be positive such that $\mathbf{q}^2 = Q^2 + \nu^2$), $A = (Q^2/\mathbf{q}^2)^2$ and $B = \tan^2(\theta/2) + Q^2/2\mathbf{q}^2$. For nuclear elastic scattering at very low \mathbf{q} on ^{12}C $Q^2 = \mathbf{q}^2$ to a good approximation.

For elastic scattering and nuclear excitations the square of the electric and magnetic form factors are obtained by the integration of the measured response functions over ν . In the experimental extractions of form factors for elastic scattering and nuclear excitations the Mott cross section is defined with an additional factor of Z^2 because both the nuclear elastic cross section and

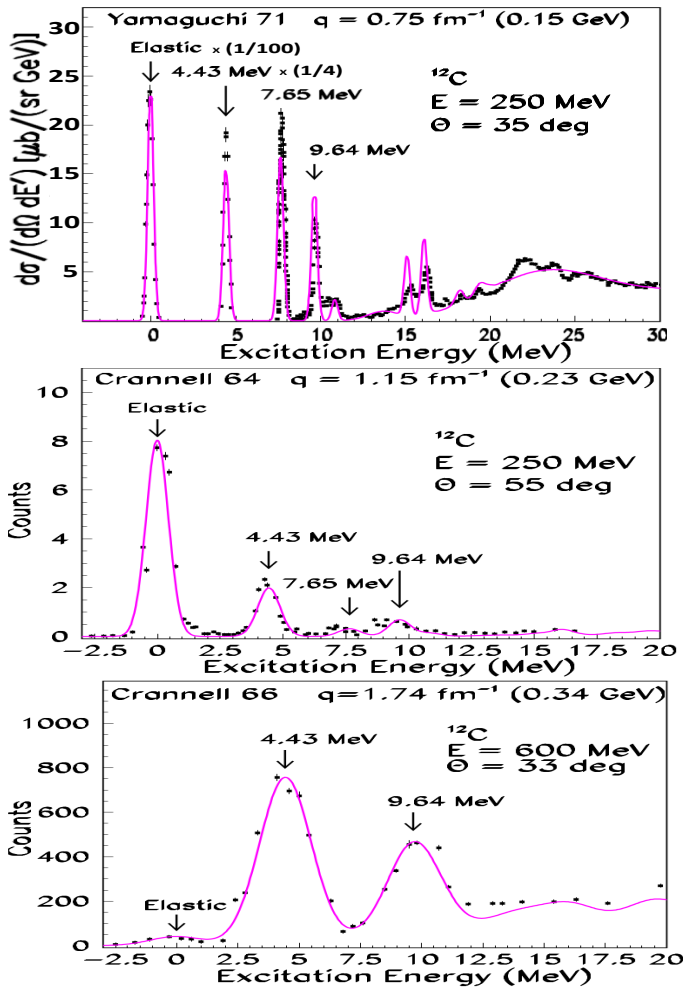


FIG. 1: **Top panel:** Radiatively corrected cross section from Yamaguchi[10](measured with high resolution of 0.25%) for the scattering of 250 MeV electrons from ^{12}C at 35° . Here, the cross section for the elastic peak has been divided by 100 and the cross section for the 4.43 MeV state by 4. **5 Middle panel:** Radiatively corrected cross section[9] (in arbitrary units) for the scattering of 250 MeV electrons from ^{12}C at 55° . **Bottom panel:** Radiatively corrected cross section[9] (in arbitrary units) for the scattering of 600 MeV electrons from ^{12}C at 33° . The peaks for elastic scattering and for the first three nuclear excitations at 4.43, 7.66 and 9.64 MeV are clearly visible. The solid curve is the predicted radiatively corrected cross section using our fits to the form factors and QE cross sections. The fit is normalized to the elastic cross section for the $E=250$ MeV and 55° data. For the $E= 600$ MeV and 33° data we normalize to the cross section for the 4.43 MeV state.

the cross sections for the the electro excitation of nuclear states are proportional to Z^2 times charge form factors $F_{iC}^2(\mathbf{q})$. Here, the subscript zero denotes the nuclear elastic peak and subscripts 1-N denote nuclear excitations. The charge form factors can be thought of as the product[11, 13] of the proton electric form factor and the form factors of the spatial distribution of protons in the

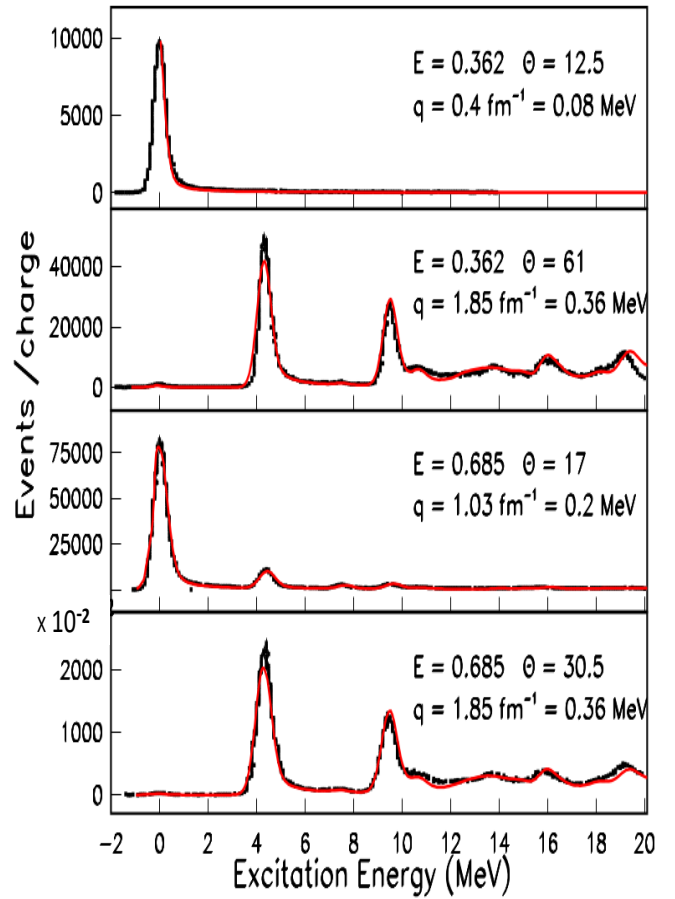


FIG. 2: Radiatively *uncorrected* cross section (in arbitrary units) from the LEDEX experiment[11] on ^{12}C . The solid red line is the radiatively *uncorrected* cross section from our fit to the form factors and QE cross sections. It is normalized to the elastic cross section at zero excitation energy for the 12.5 and 17.0 degree data, and to the cross section for the 4.43 MeV state for the 30.5 and 61.0 degree data.

nucleus.

III. COULOMB SUM RULE

The inelastic Coulomb Sum Rule is the integral of $R_L(\mathbf{q}, \nu)d\nu$, *excluding the elastic peak and pion production processes*. It has contributions from QE scattering and from electro-excitations of nuclear states:

$$\begin{aligned}
 \text{CSR}(\mathbf{q}) &= \int R_L(\mathbf{q}, \nu)d\nu \\
 &= \int R_L^{\text{QE}}(\mathbf{q}, \nu)d\nu + G_E^{\prime 2}(Q^2) \times Z^2 \sum_{\text{all}}^L F_i^2(\mathbf{q}) \\
 &= G_E^{\prime 2}(Q^2) \times [Z \int V_L^{\text{QE}}(\mathbf{q}, \nu)d\nu + Z^2 \sum_{\text{all}}^L F_i^2(\mathbf{q})].
 \end{aligned} \tag{3}$$

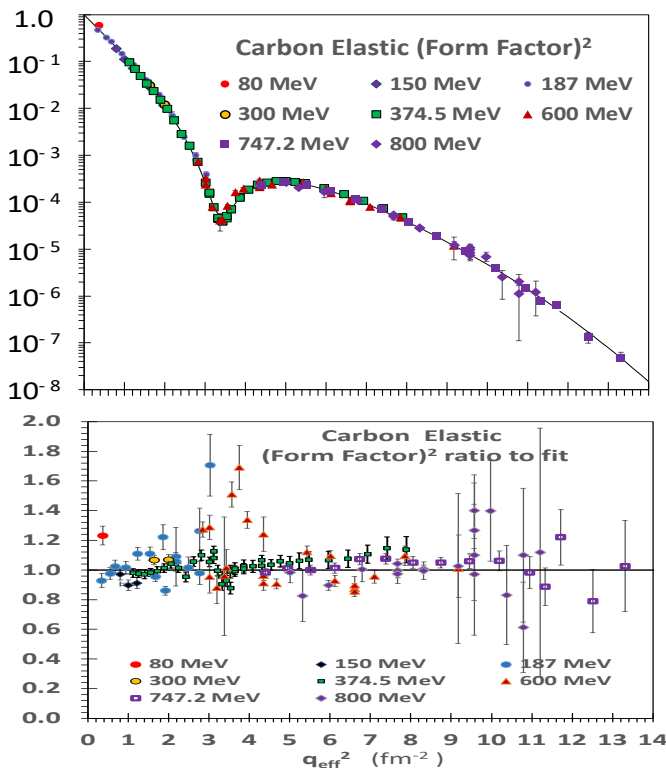


FIG. 3: **Top panel:** Measurements[17] of the nuclear elastic longitudinal charge form factor (squared) for ^{12}C versus q_{eff}^2 . **Bottom panel:** Ratio to our fit.

We define $V^{QE}(\mathbf{q}, \nu)$ as the reduced longitudinal QE response, which integrates to unity in the absence of any suppression (e.g. Pauli blocking). The charge form factors for the electro-excitation of nuclear states $F_{iC}^2(\mathbf{q})$ is related to $F_i^2(\mathbf{q})$ by the expression $F_{iC}^2(\mathbf{q}) = G_{Ep}^{\prime 2}(Q^2) \times F_i^2(\mathbf{q})$. In order to account for the small contribution of the neutron and relativistic effects $G_E^{\prime 2}(Q^2)$ is given by[12]:

$$G_E^{\prime 2}(Q^2) = [G_{Ep}^2(Q^2) + \frac{N}{Z} G_{En}^2(Q^2)] \frac{1 + \tau}{1 + 2\tau}, \quad (4)$$

where, G_{Ep} and G_{En} are the electric form factors [14] of the proton and neutron, respectively and $\tau = Q^2/4M_p^2$. By dividing Eq. 3 by $ZG_E^{\prime 2}(\mathbf{q})$ we obtain the normalized inelastic Coulomb Sum Rule $S_L(\mathbf{q})$:

$$S_L(\mathbf{q}) = \int V_L^{QE}(\mathbf{q}, \nu) d\nu + Z \sum_{\text{all}}^L F_i^2(\mathbf{q}). \quad (5)$$

IV. PARAMETERIZATION OF ^{12}C NUCLEAR ELASTIC AND NUCLEAR EXCITATION FORM FACTORS

A. ^{12}C elastic form factor versus q_{eff}^2

The ^{12}C nucleus has a spin parity of 0^+ . We fit the measured ^{12}C elastic longitudinal (charge) form factor with the following functional form:

$$F_{oC}^2(\mathbf{q}_{\text{eff}}^2) = \frac{1 + 1.5 \times 10^{-3} \mathbf{q}_{\text{eff}}^4}{1 + e^{\text{Power}}} [H^2(\mathbf{q}_{\text{eff}}^2) + G(\mathbf{q}_{\text{eff}}^2)] \quad (6)$$

Here, $\text{Power} = \frac{\mathbf{q}_{\text{eff}}^2 - 12.0}{1.4}$ is included to better describe the form factor at very large \mathbf{q} . The effective[15] \mathbf{q}^2 is

$$\mathbf{q}_{\text{eff}}^2 = \mathbf{q}^2 (1 + 4Z\alpha / (3\langle r^2 \rangle E))$$

Which for carbon is $\mathbf{q}_{\text{eff}}^2 = \mathbf{q}^2 (1 + 0.00465/E)^2$ (where E is in GeV). The function $H(\mathbf{q}_{\text{eff}}^2)$ is the harmonic well shape with ($\alpha = 1.21$, and $a_0 = 1.65$). It is given by[16]:

$$H(\mathbf{q}_{\text{eff}}^2) = [1 - \frac{\alpha \mathbf{q}_{\text{eff}}^2 a_0^2}{2(2 + 3\alpha)}] \exp[\frac{-\mathbf{q}_{\text{eff}}^2 a_0^2}{4}], \quad (7)$$

The function $G(\mathbf{q}_{\text{eff}}^2)$ fills in the dip in the location of the diffraction minimum.

$$G(\mathbf{q}_{\text{eff}}^2) = 5.0 \times 10^{-5} e^{-[(\mathbf{q}_{\text{eff}}^2 - 3.1)/0.66]^2}$$

In the above parametrization $\mathbf{q}_{\text{eff}}^2$ is in units of fm⁻². A comparison of the parametrization of the nuclear elastic charge form factor for ^{12}C to experimental data[17] is shown on the top panel of Fig. 3. The ratio of the measurements to the fit is shown on the bottom panel.

B. Form factors for nuclear excitations in ^{12}C

We begin by parameterizing the measurements of the longitudinal and transverse form factors for the electro-excitation of all nuclear states in ^{12}C with excitation energies (E_x) less than 16.0 MeV (the approximate proton removal energy from ^{12}C). For these states the measurements are straightforward since the QE cross section is zero for $E_x < 16$ MeV. Note that unlike the nuclear elastic form factor which is equal to 1.0 at $\mathbf{q}=0$, all longitudinal form factors for nuclear excitations must vanish at $\mathbf{q}=0$.

1. ^{12}C excitation form factors for the 4.44 MeV and 9.64 MeV states

The longitudinal form factors (squared) for the electro excitation of the 4.44 and 9.64 MeV nuclear excited states are parametrized as $F_{iC}^2(\mathbf{q}_{\text{eff}}^2)$ where

$$F_{iC}^2(\mathbf{q}_{\text{eff}}^2) = \frac{(\mathbf{q}_{\text{eff}}^2)^3}{(\mathbf{q}_{\text{eff}}^2)^3 + d} \sum_{j=1}^{j=3} N_j e^{-[(\mathbf{q}_{\text{eff}}^2 - C_j)/\sigma]^2} \quad (8)$$

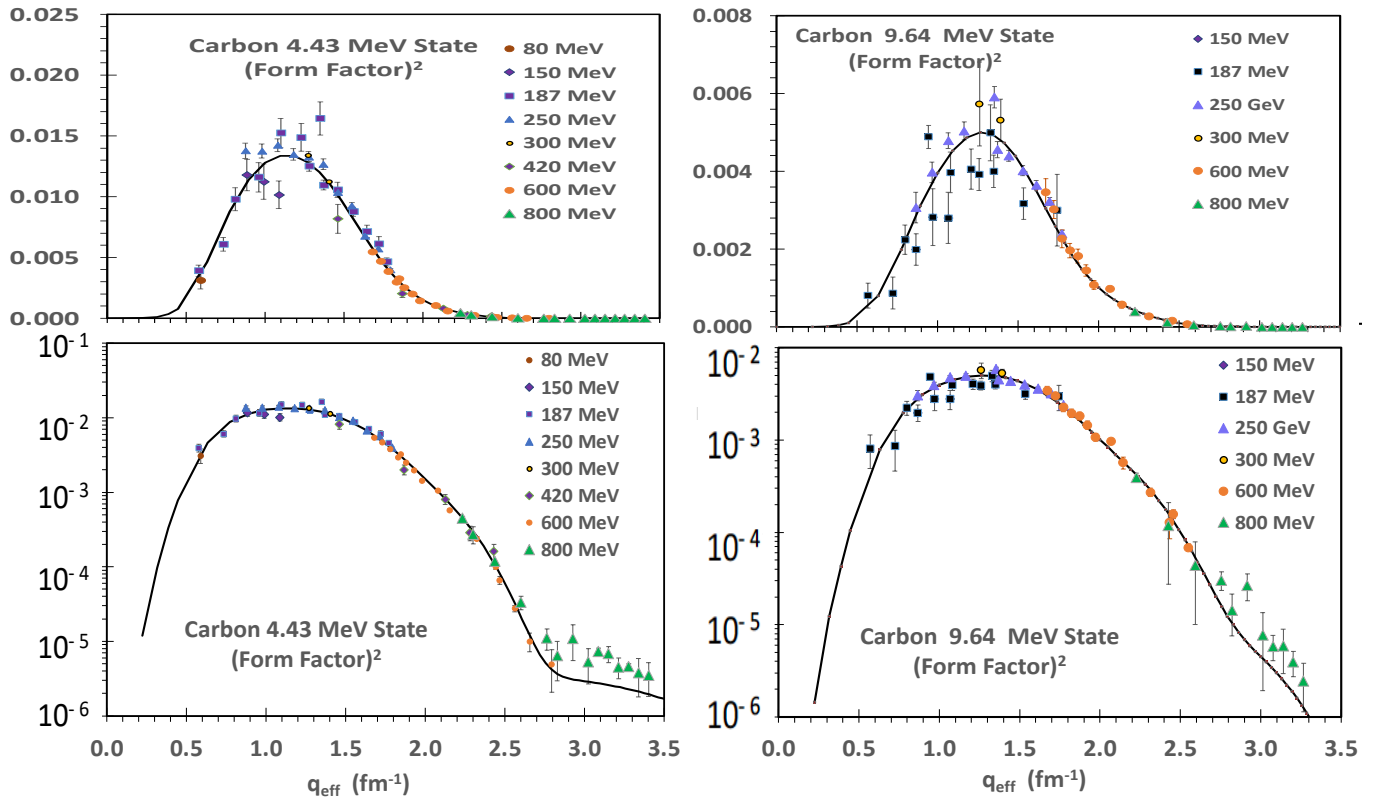


FIG. 4: Measurements[17] of the longitudinal charge form factors (squared) for the 4.43 MeV state (left) and the 9.64 MeV state (right) in ^{12}C . The form factors (squared) are shown on linear scales and logarithmic scales on the top and bottom panels, respectively.

State	N_1	C_1	σ_1	N_2	C_2	σ_2	N_3	C_3	σ_3	d	Data from Ref.
4.44 MeV 2^+L ($\mathbf{q}_{\text{eff}}^2$)	1.41×10^{-2}	1.125	1.71	7.0×10^{-4}	3.70	1.6	3.3×10^{-6}	6.5	7.0	0.10	[17]
9.64 MeV 3^-L ($\mathbf{q}_{\text{eff}}^2$)	5.00×10^{-3}	1.46	1.60	6.6×10^{-4}	3.46	2.0	7.0×10^{-6}	7.0	2.8	0.20	[17]

TABLE I: Parameters of our fits (eq. 8) to the ^{12}C longitudinal charge form factors (squared) for the 4.44 and 9.64 MeV nuclear excited states in ^{12}C . For these states, the parametrizations are in terms of $\mathbf{q}_{\text{eff}}^2$ in units of fm^{-2} . Here $\mathbf{q}_{\text{eff}}^2 = \mathbf{q}^2 \times (1 + 0.00465/E)^2$, where E is in GeV[15].

Here \mathbf{q}^2 is in units of fm^{-2} . The parameters for the 4.44 and 9.64 MeV states are given in Table I. Comparisons of our parametrizations of the excitation form factors (squared) for the 4.44, and 9.64 MeV states to experimental data[17] are shown in Figure 4.

2. ^{12}C form factor for the 7.65 MeV state

Measurements of the square of the longitudinal form factor versus \mathbf{q}_{eff} (in units of fm^{-1}) for the 7.65 MeV state in ^{12}C are shown in Fig. 5 on linear and logarithmic scales. The solid line is a fit using the functional form[18]

described below.

$$F^2(\mathbf{q}_{\text{eff}}) = \left[\frac{1}{Z} e^{-\frac{1}{2}(b\mathbf{q}_{\text{eff}})^2} \sum_{n=1}^5 c_n (b\mathbf{q}_{\text{eff}})^{2n} \right]^2 \quad (9)$$

The fit parameters are $b = 1.3457 \text{ fm}$, $c_1 = +0.52$, $c_2 = -0.25 \times 10^{-1}$, $c_3 = -0.7 \times 10^{-2}$, $c_4 = +0.5 \times 10^{-3}$ and $c_5 = -0.5 \times 10^{-4}$.

The data for incident energies between 31-59 MeV (taken at Darmstadt) are published[19]. The 243 MeV and 428 MeV data (taken at NIKHEFF) are available in a PhD Thesis[20]. The 140-370 MeV data (taken at Bates) are unpublished[21]. The 375 MeV data (taken at Stanford HEPL) are unpublished[22]. The 187+250 MeV data[23] and the 187 MeV data[24] (taken at the Stanford Linear Accelerator) are published.

State	N_1	C_1	σ_1	N_2	C_2	σ_2	N_3	C_3	σ_3	a	b	Ref.
10.84 MeV 1⁻L	5.0×10^{-4}	1.0	0.3	8.0×10^{-4}	1.4	0.4	-	-	-	-	-	[25]
11.83 MeV 2 ⁻ T	3.9×10^{-5}	1.2	0.5	1.2×10^{-5}	2.0	0.4	-	-	-	-	-	[28]
12.71 MeV 1 ⁺ T	3.0×10^{-6}	0.63	0.4	1.0×10^{-8}	1.0	0.1	2.0×10^{-6}	1.8	0.6	2.5×10^{-5}	1	[26]
13.7 MeV 4⁻L $\sigma=1.25$ MeV	4.0×10^{-4}	1.0	0.35	1.0×10^{-3}	1.75	0.45	4.0×10^{-4}	0.85	0.65	-	-	[9-11]
14.08 MeV 4⁺L	2.4×10^{-5}	1.8	0.6	-	-	-	-	-	-	-	-	[27]
15.1 MeV 1⁺L 15.1 MeV-T	6.0×10^{-4} 2.5×10^{-4}	0.85 0.63	0.7 0.4	- 2.8×10^{-4}	- 0.84	- 0.2	- 2.4×10^{-5}	- 2.0	- 0.5	- 2.5×10^{-5}	- 1	[26] [26]
16.1 MeV 2⁺L 16.1 MeV 2 ⁺ T	12.0×10^{-4} 5.9×10^{-4}	1.05 1.2	0.6 0.55	- 2.4×10^{-4}	- 2.2	- 0.6	- -	- -	- -	- -	- -	[10]
16.6 MeV 2 ⁻ T	2.6×10^{-4}	1.6	0.6	5.0×10^{-5}	2.5	0.35	-	-	-	-	-	[10][28]
18.1 MeV 1 ⁺ T	1.9×10^{-4}	0.8	0.35	1.8×10^{-4}	1.25	0.45	-	-	-	-	-	[10][28]
18.6 MeV-L	3.2×10^{-4}	1.3	0.5	-	-	-	-	-	-	-	-	[10]
19.3 MeV 2 ⁻ T	1.02×10^{-3}	1.32	0.77	3.75×10^{-4}	1.7	0.6	1.0×10^{-4}	2.2	0.3	3.6×10^{-4}	1	[10][28]
20.0 MeV 2⁺L	1.6×10^{-4}	1.2	0.42	1.6×10^{-5}	1.8	0.4	-	-	-	-	-	[10]
20.6 MeV 3 ⁻ T	1.9×10^{-4}	1.45	0.5	5.5×10^{-5}	2.1	0.4	-	-	-	-	-	[10][28]
(21-26 MeV) 23.0 MeV-L $\sigma=4.75$ MeV 23.0 MeV-T	2.8×10^{-3} 1.83×10^{-3}	0.60 0.8	0.15 0.36	6.9×10^{-3} 1.0×10^{-4}	0.84 1.5	0.55 0.5	- -	- -	- -	- -	- -	[10] [10]
(26-37 MeV) 31.5 MeV-L $\sigma=9$ MeV 31.5 MeV-T	4.7×10^{-3} 9.0×10^{-4}	1.0 0.35	0.48 0.3	- -	- -	- -	- -	- -	- -	- -	- -	[10] [10]
(30-50 MeV) 42 MeV-L $\sigma=12$ MeV Extra Strength	2.6×10^{-3}	1.49	0.7	-	-	-	-	-	-	-	-	

TABLE II: Parameterizations of the Longitudinal (L) and Transverse (T) ^{12}C nuclear excitation form factors (squared) for the 7.65 MeV state and for states with excitation energy above 10 MeV. Unlike the parametrizations in Table I for the 4.44 and 9.64 MeV states which are functions of the square of the 3-momentum transfer $\mathbf{q}_{\text{eff}}^2$ in units of fm^{-2} , the parametrizations for the states in this table are functions of \mathbf{q}_{eff} in units of fm^{-1} . Here $\mathbf{q}_{\text{eff}}^2 = \mathbf{q}^2 \times (1 + 0.00465/E)^2$, where E is in GeV[15].

3. ^{12}C form factors for states with excitation energies above 10 MeV

The charge form factors (squared) for the electro-excitation of t states with excitation energies above 10 MeV are parameterized as $F_{iC}^2(\mathbf{q}) = \text{Max}(0.0, g_i^2)$ where

$$g_i^2(\mathbf{q}_{\text{eff}}) = \sum_{j=1}^{j=3} N_j e^{-[(\mathbf{q}_{\text{eff}} - C_j)/\sigma]^2} - a e^{-b\mathbf{q}_{\text{eff}}}. \quad (10)$$

Here, \mathbf{q}_{eff} is in units of fm^{-1} . The parameters are given in Table II. (Note that these states are parameterized versus \mathbf{q}_{eff} , while the 4.44 and 9.64 MeV states are parameterized versus $\mathbf{q}_{\text{eff}}^2$).

4. ^{12}C form factors for states with excitation energies above 10 MeV and below 16 MeV

We use equation 10 to parameterize the form factor for excitation energy of 10.84 MeV[25], and also for excitation energies of 12.71, 14.09 and 15.11 MeV[26, 27]. In addition, we find that published differential cross section measurements indicate that there is an additional longitudinal continuum in the region between 12 to 15 MeV. We parameterize this longitudinal continuum as one broad state at 13.7 MeV ($\sigma=1.25$ MeV). For the transverse form factors in this region we parameterize the data of Hicks84[28].

5. ^{12}C form factors for states with excitation energies above 16 MeV

Initially, we parameterize the longitudinal and transverse form factors measured by Yamaguchi71[10] for

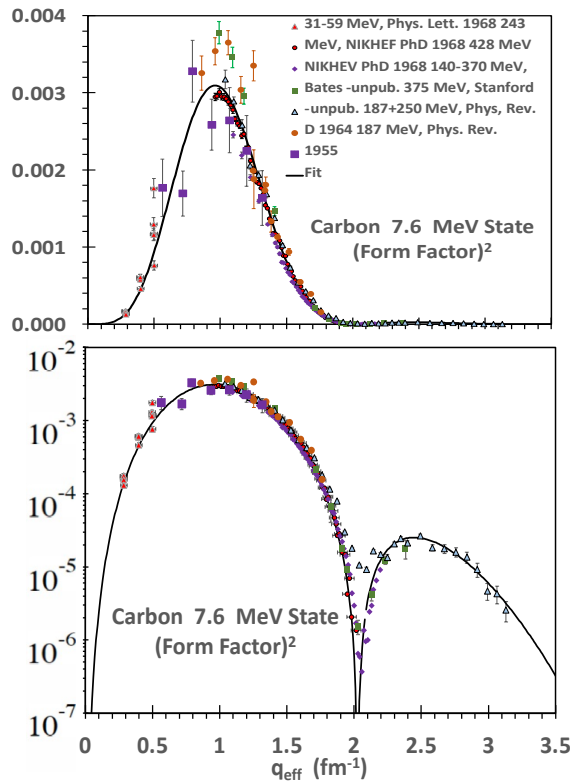


FIG. 5: Measurements of the longitudinal charge form factor (squared) for the 7.65 MeV state shown on linear (top) and logarithmic (bottom) scales. The solid line is the fit described in the text.

states with excitation energies above 16 MeV. However, in the Yamaguchi71 analysis the contributions from quasielastic (QE) scattering are not subtracted. Therefore, We perform a reanalysis of the Yamaguchi71 data in combination of all published cross sections with $16 < E_x < 55$ MeV. We subtract the QE contribution using our QE model[2] (which includes superscaling[29] with Rosenfelder[30] Pauli Suppression) and extract updated longitudinal and transverse form factors. For $E_x > 20$ MeV (region of the Giant Dipole resonances) we group the strength from multiple excitations into a three states with a large width in E_x and extract effective form factors accounting for all states in these regions. The updated parameters are given in Table II.

The longitudinal and transverse response functions for ^{12}C , $R_L(\mathbf{q}, E_x)$ and $R_T(\mathbf{q}, E_x)$, extracted by Yamaguchi71[10] for excitation energies above 16 MeV and less than 40 MeV are shown in Figure 6 (black points). Also shown are $R_L(\mathbf{q}, E_x)$ and $R_T(\mathbf{q}, E_x)$ extracted from our universal fit to all electron scattering cross section data on ^{12}C (solid red line). The QE contribution to the total response functions is shown as the dashed red line. An estimated resolution smearing of 600 keV has been applied to the excitations in the fit to match the data. While individual states are well reproduced at

low excitation energy, above E_x of 20 MeV the effect of grouping several excitations together into three broad effective states in the fit can be seen. While the fit does not capture the structure from individual states above 20 MeV, the total strength is seen to be well reproduced.

C. Comparison to ^{12}C experimental data for excitation energies below 50 MeV

Experimental radiatively corrected inelastic electron scattering cross sections on ^{12}C for excitation energies less than 50 MeV are shown in Figure 7. Also shown are the corresponding cross sections from our universal fit to all ^{12}C data. The cross sections for excitation energies less than 12 MeV are multiplied by (1/6). The pink solid line is the predicted total cross section from our universal fit[2] which include the contributions from all sources (nuclear excitation form factors, quasielastic scattering and pion production processes). The QE contribution is shown as the dashed blue line and the "Transverse Enhancement/Meson Exchange Currents" contribution is shown as the dot-dashed line. Details of the fit are described in reference[2]. Most of the cross section measurements are from Yamaguchi71[10]. The cross sections for $E_o=54$ MeV at 180° are from Goldemberg64[31] and the the cross sections for $E_o=65$ MeV at 180° are from deForest65[32]. The measurements at 180° are only sensitive to the transverse form factors.

V. ANALYSIS OF ^{16}O EXCITED STATES

A. ^{16}O excited states with $E_x < 12.5\text{MeV}$

In order to minimize correlations between our parameterizations of the form factors for the nuclear excitations in ^{12}C and ^{16}O we parameterize the form factors for ^{16}O states using a somewhat different functional form. The form factors for the nuclear excited states in ^{16}O are parameterized as $F_{iC}^2(\mathbf{q}^2) = \text{Max}(0.0, g_i^2)$ where

$$g_i^2(\mathbf{q}_{\text{eff}}^2) = \mathbf{q}_{\text{eff}}^2 \times \left[\sum_{j=1}^{j=3} N_j e^{-[(\mathbf{q}_{\text{eff}}^2 - C_j)/\sigma]^2} - a e^{-b\mathbf{q}_{\text{eff}}^2} \right]. \quad (11)$$

Here, $\mathbf{q}_{\text{eff}}^2$ is in units of fm^{-2} .

The form factors for nuclear excitations in ^{16}O with excitation energies below proton removal threshold (about 12 MeV) are easily measured because there is no contribution from QE scattering in this region. The nine longitudinal form factors (squared) in ^{16}O for excitation energies below 12.5 MeV are shown in Figures 8, 9 and 10 on linear (top panels) and logarithmic (bottom panels) scales. The data in the figures are from Buti-86[33]. The solid blue lines are our parameterizations using the parameters listed in Table III.

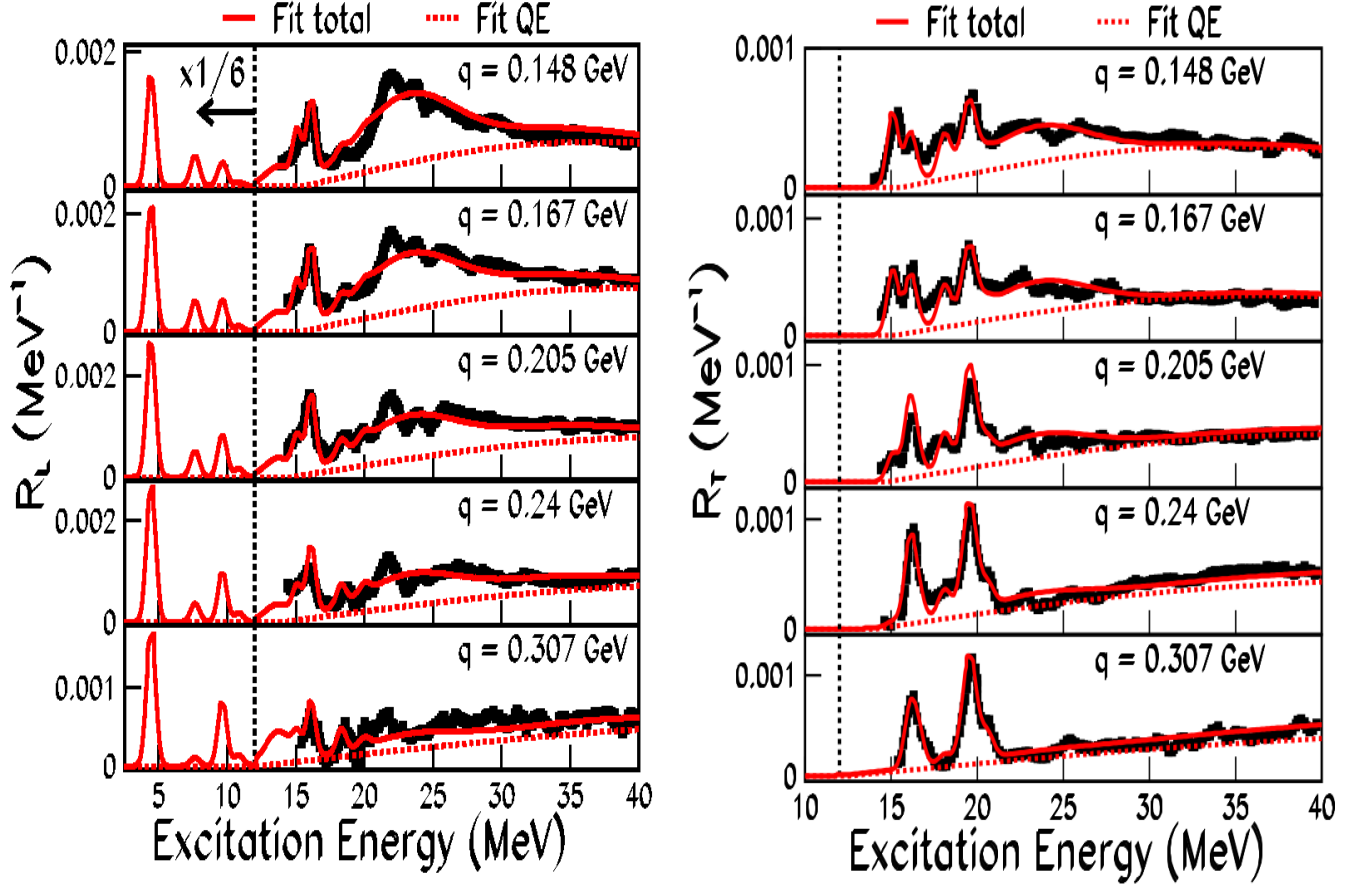


FIG. 6: Comparison of the longitudinal (R_L , left) and transverse (R_T , right) response functions for ^{12}C extracted by Yamaguchi 71[10] (black squares) to the response functions extracted from our universal fit to all available electron scattering cross section data on ^{12}C (solid red line). The contributions from excitation energies less than 12 MeV are multiplied by $(1/6)$. The QE contribution to the total response functions is represented by the red dashed line. In our fit, we model the response functions for all states the region of the Giant Dipole Resonance (20-30 MeV) region as one average broad excitation.

State	MeV	N_1	C_1	σ_1	N_2	C_2	σ_2	N_3	C_3	σ_3	a	b	Ref.
$0_2^+ L$	6.0494	0.70	0.35	0.58	0.120	1.20	0.500	0.0050	4.30	1.60	0.220	6.00	Buti-86
$3_1^- L$	6.1299	1.60	1.00	0.45	4.100	1.07	1.700	0.2000	2.55	2.40	3.100	1.10	Buti-86
$2_1^+ L$	6.9171	6.50	0.20	0.75	1.000	1.10	0.955	0.0032	5.30	1.35	5.000	2.50	Buti-86
$1_1^- L$	7.1169	0.95	0.94	0.68	0.800	1.50	1.200	0.1000	2.40	1.55	0.400	3.00	Buti-86
$2_2^+ L$	9.8445	0.10	0.70	0.65	0.080	1.70	1.200	0.0120	2.50	2.0	0.007	2.000	Buti-86
$4_1^+ L$	10.3560	0.09	1.30	0.70	0.087	2.05	1.200	0.0140	3.30	1.7	0.007	2.000	Buti-86
$4_2^+ L$	11.0967	0.04	1.10	0.85	0.042	2.20	1.100	0.0110	3.20	1.9	0.000	10.000	Buti-86
$2_3^+ L$	11.5200	2.00	0.50	0.60	0.600	1.00	1.050	0.0040	5.30	1.4	0.007	1.657	Buti-86
$0_3^+ L$	12.0490	1.15	0.20	0.95	0.050	1.50	0.850	0.0015	5.20	1.3	1.00	4.00	Buti-86
	12.5-20.0	2.00	0.35	0.30	8.000	0.0	1.90	-	-	-	0.007	1.66	Hotta74
	20.0-35.0	18.00	0.00	0.40	7.000	0.6	0.80	2.5000	1.0	1.5	-	-	Hotta74
	35.0-55.0	0.8	0.00	0.30	1.300	0.6	3.00	-	-	-	0.004	1.66	use <i>carbon</i>

TABLE III: Parameterizations of the square of the longitudinal (L) nuclear excitation form factors in ^{16}O (in units of 10^{-3}). Data taken from Buti-86[33] and Hotta74[34]. The parameterizations are functions of $\mathbf{q}_{\text{eff}}^2$ in units of fm^{-2} .

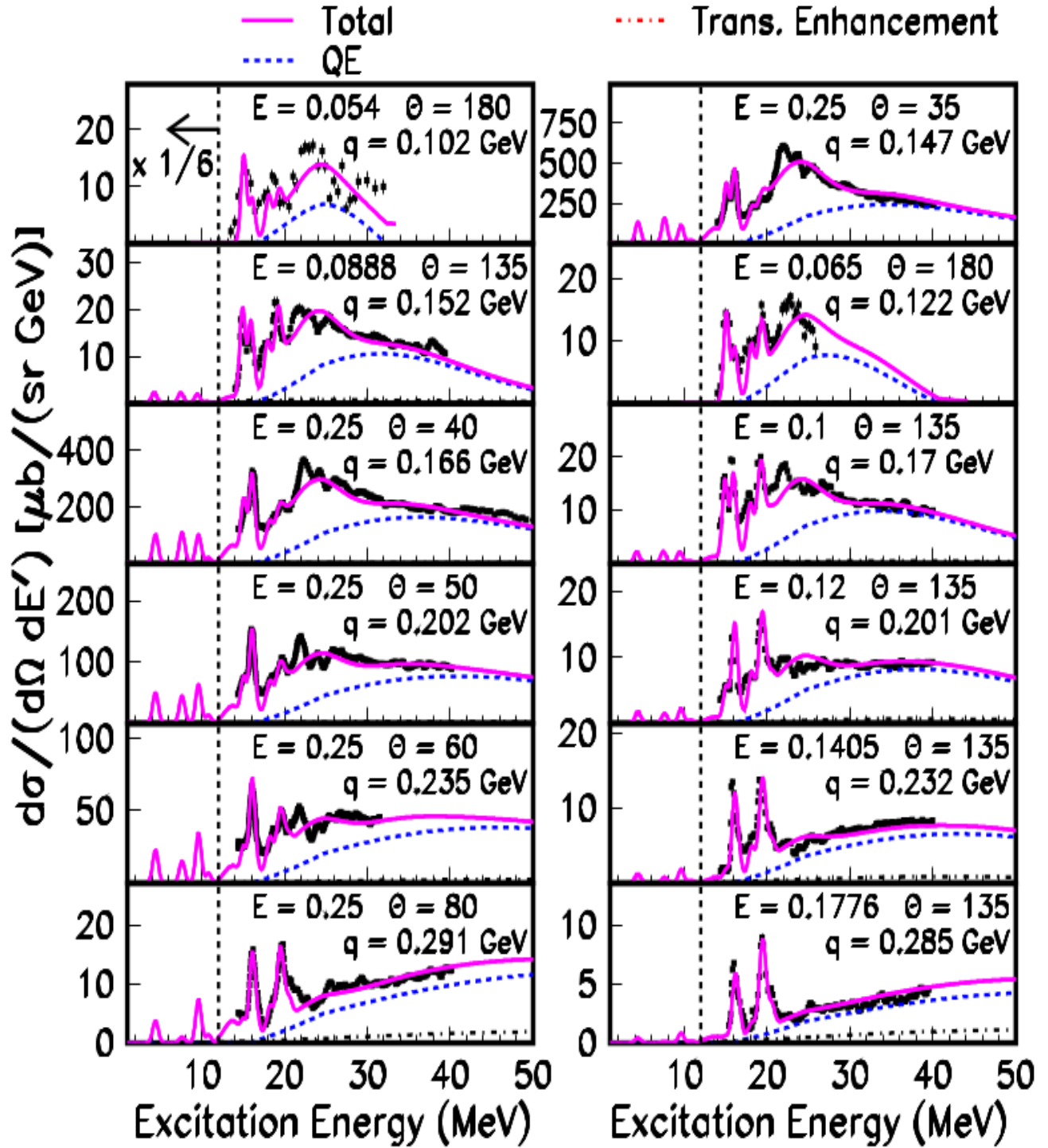


FIG. 7: Radiatively corrected inelastic electron scattering cross sections on ^{12}C for excitation energies less than 50 MeV. The cross sections for excitation energies less than 12 MeV are multiplied by $(1/6)$. The pink solid line is the predicted total cross section from our universal fit[2] to all electron scattering data on ^{12}C . The fit include nuclear excitations, a superscaling QE model[29] with Rosenfelder Pauli suppression[30] (dashed blue line), "Transverse Enhancement/Meson Exchange Currents" (dot-dashed line) and pion production processes (at higher excitation energies). The data are from Yamaguchi71[10] except for the cross sections for $E_o=54$ MeV and 180° (from Goldemberg64[31]) and the cross sections for $E_o=65$ MeV and 180° (from deForest65[32]). The measurements at 180° are only sensitive to the transverse form factors.

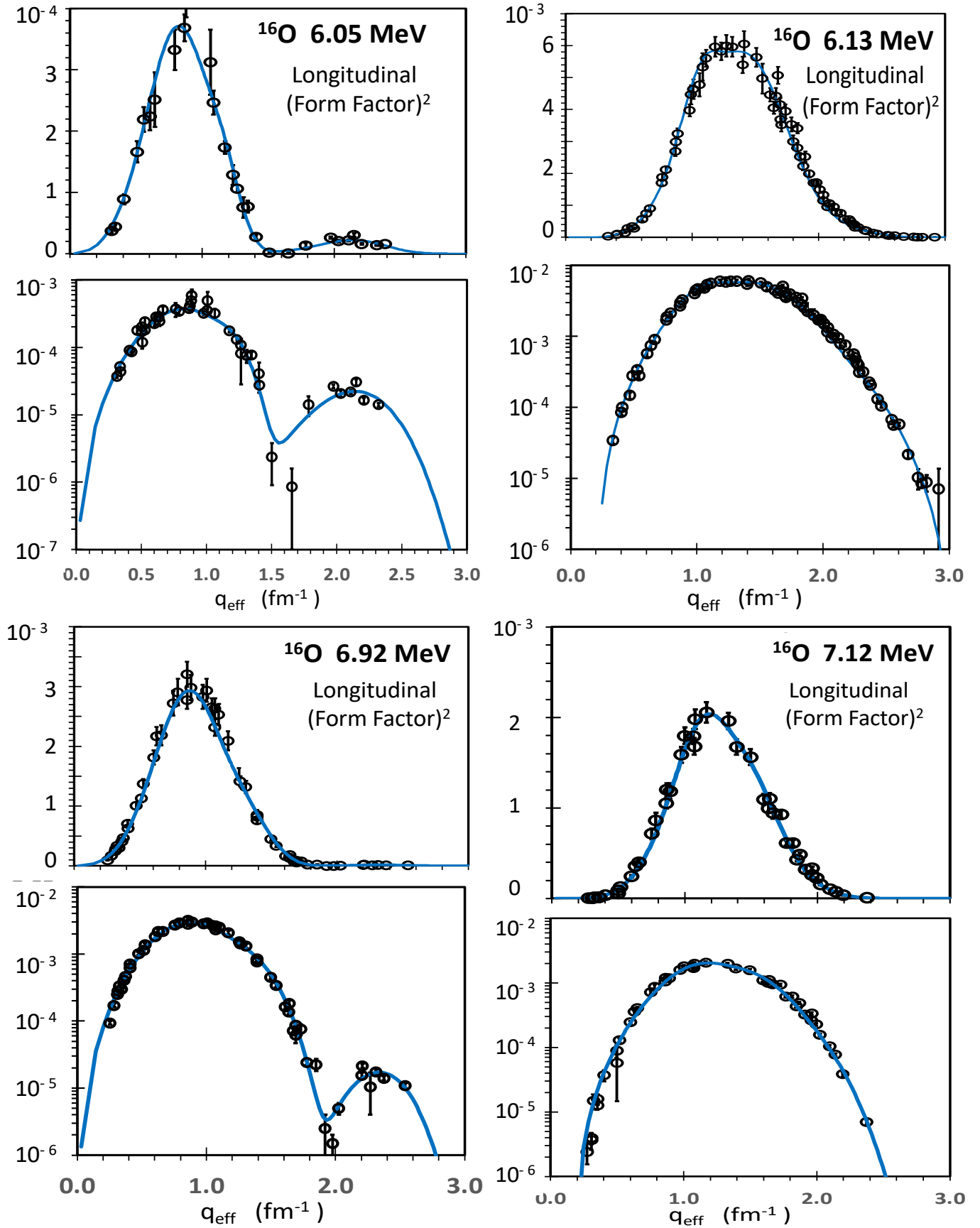


FIG. 8: The square of the longitudinal form factors in ^{16}O for nuclear excitations of 6.05, 6.23, 6.92 and 7.12 MeV on linear (top panels) and logarithmic (bottom panels) scales. The data are from Buti-86[33]. The blue solid lines are our parameterizations from Table III.

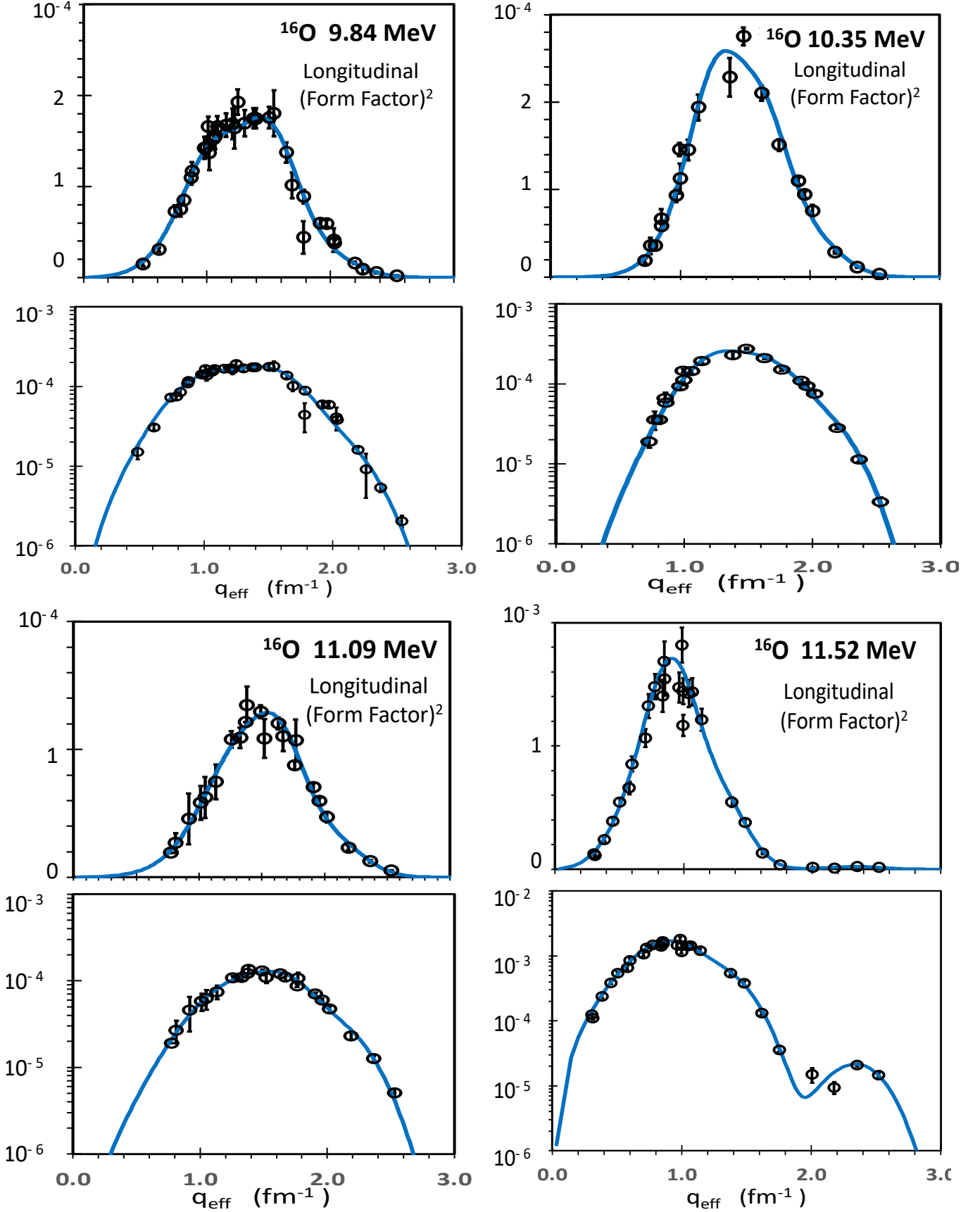


FIG. 9: The square of the longitudinal form factors in ^{16}O for nuclear excitations of 9.84, 10.35, 11.09 and 11.52 MeV on linear (top panels) and logarithmic (bottom panels) scales. The data are from Buti-86[33]. The blue solid lines are our parameterizations from Table III.

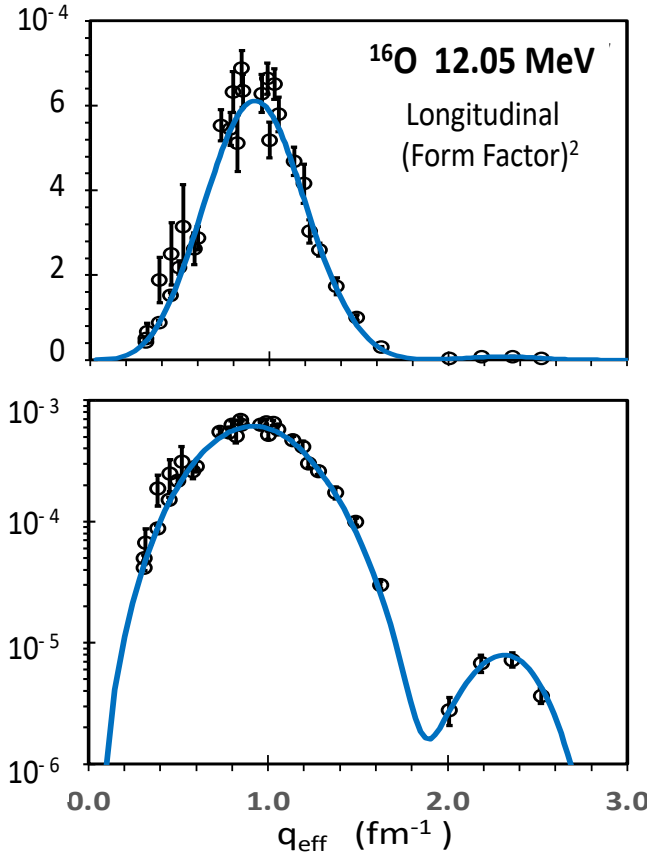


FIG. 10: The square of the longitudinal form factors in ^{16}O for nuclear excitation of 12.5 MeV on linear (top panel) and logarithmic (bottom panel) scales. The data are from Buti-86[33]. The blue solid lines are our parameterizations from Table III.

B. ^{16}O excited states with $E_x > 12.5\text{MeV}$

For excitation energy above 12.5 MeV there is a significant contribution from QE scattering. Here we group the states in two regions of excitation energy (12.5-20 MeV and 20-35 MeV).

The top row in Fig. 11 shows the longitudinal response function $R_L(\mathbf{q}, E_x)$ for ^{16}O from Hotta74[34] for three values of \mathbf{q} . The solid red line is the original estimate of the QE contribution used in the Hotta74 publication. The solid green line is the QE contribution determined using the QE parameters from our universal fit to all ^{12}C data. We find that the QE cross section predictions for ^{16}O using the parameters from the ^{12}C fit also describe all (but limited) available data on ^{16}O as shown in [2]. We use the Hotta74 data to extract the longitudinal form factors for the nuclear excitation in ^{16}O in the 12.5-20 MeV and the 20-35 MeV groupings in excitation energy.

The middle and bottom rows in Fig. 11 show the extracted longitudinal form factor for the 12.5-20 MeV and

20-35 MeV groupings in excitation energy on linear (middle) and logarithmic (bottom) scales. Also shown is the form factor measurement from Goldman70[35]. The longitudinal form factor measured by Goldman70 for the 20-30 MeV grouping in excitation energy has been corrected by subtracting the QE contribution (from our universal fit) and extending the excitation range to 20-35 MeV.

Since no data are available for the form factor for nuclear excitations the 36-55 MeV region in ^{16}O we assume that the form factor for ^{16}O is the same as the form factor for ^{12}C in this region.

VI. CONTRIBUTION OF NUCLEAR EXCITATIONS TO $S_L(\mathbf{q})$ IN ^{12}C AND ^{16}O

The contributions of nuclear excitation to $S_L(\mathbf{q})$ (Eq. 5) in ^{12}C and ^{16}O are calculated using the form factor parameterizations given in Tables I, II and III. The left side panels of Figures 12 and 13 show the contributions of nuclear excitations (with excitation energies below 10 MeV, 20.5 MeV, 30 MeV and 55 MeV) to $S_L(\mathbf{q})$ for ^{12}C and ^{16}O , respectively.

The total contribution to $S_L(\mathbf{q})$ can be parametrized as follows:

$$\begin{aligned}
 Z \sum_{all} F_i^2(\mathbf{q}) &= N_1 \exp((x - C_1)^2/D_1^2) \\
 &+ N_2 \exp(-(x - C_2)^2/D_2^2) \\
 &+ N_3 \exp(-(x - C_3)^2/D_3^2) \quad (12)
 \end{aligned}$$

where $x = \mathbf{q}/K_F$. For ^{12}C $K_F = 0.228$ GeV, $N_1 = 0.260$, $C_1 = 1.11$, $D_1 = 0.50$, $N_2 = 0.075$, $C_2 = 0.730$, $D_2 = 0.30$, and $N_3 = 0.01$, $C_3 = 2.0$, $D_3 = 0.30$. The fit and the data are shown on the right side panel of Fig. 12.

For ^{16}O $K_F = 0.228$ GeV, $N_1 = 0.240$, $C_1 = 1.07$, $D_1 = 0.48$, $N_2 = 0.073$, $C_2 = 0.70$, $D_2 = 0.37$, and $N_3 = 0.039$, $C_3 = 1.55$, $D_3 = 0.50$. The fit and the data are shown on the right side panel of Fig. 13.

The left panel of Fig. 14 shows a comparison of the contributions of all excited states to the $S_L(\mathbf{q})$ for ^{12}C and ^{16}O . The uncertainty in the total contribution of the excited states for both nuclei is 0.01 plus 10% added in quadrature. These results indicate that the total contribution of nuclear excitations to $S_L(\mathbf{q})$ in ^{16}O is consistent with being equal to the total contribution of nuclear excitations to $S_L(\mathbf{q})$ in ^{12}C within errors. The total contribution of all states with excitation energy below 55 MeV is largest at $\mathbf{q} = 0.22$ GeV, where it reaches a maximum of 0.29 ± 0.03 .

VII. UPDATED EXTRACTION OF $S_L(\mathbf{q})$ FOR ^{12}C AND ^{16}O

In our previous paper[2] we performed a fit to all electron scattering data on ^{12}C and ^{16}O . We found that

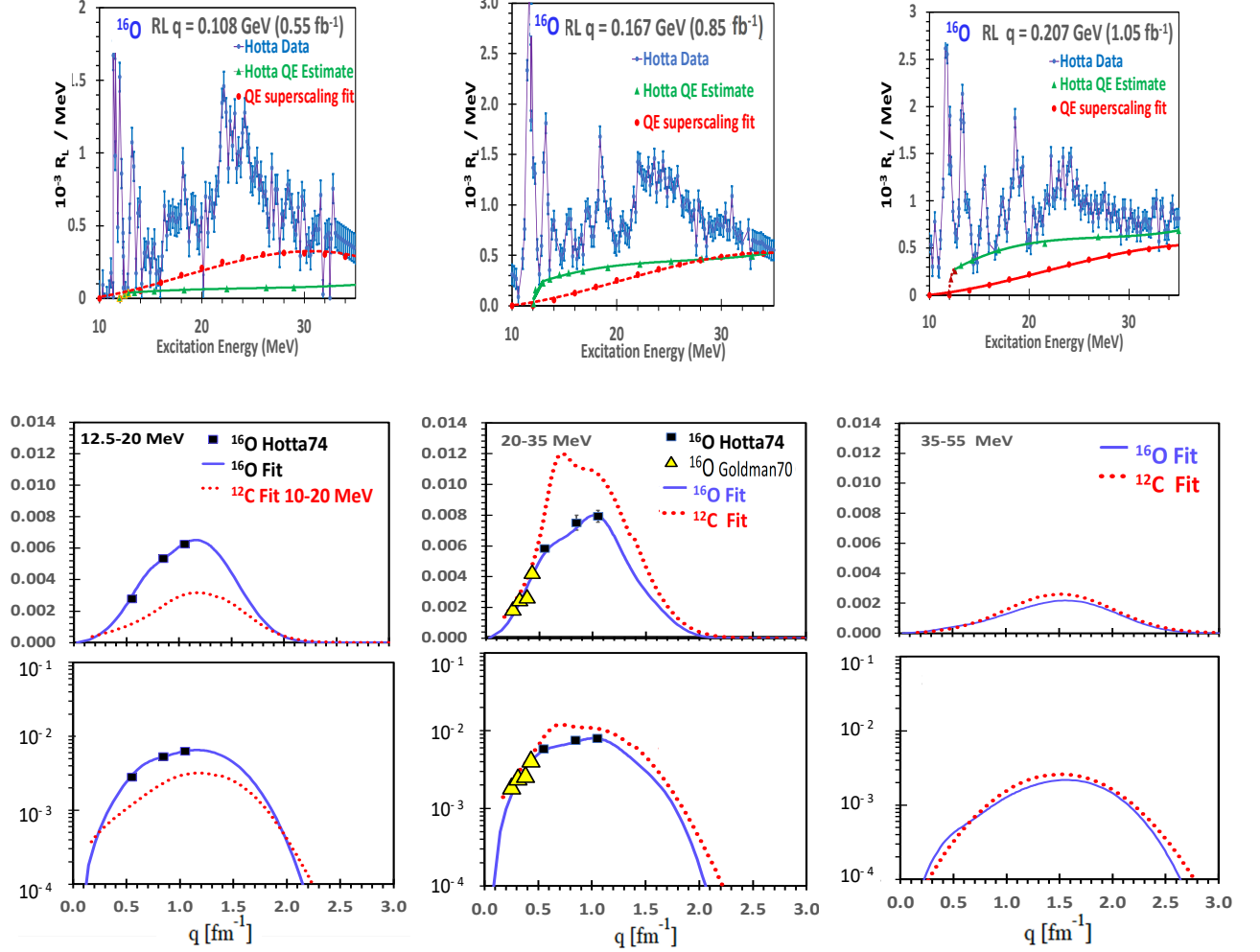


FIG. 11: **Top row:** The longitudinal response function $R_L(\mathbf{q}, E_x)$ for ^{16}O from Hotta74[34] for three values of \mathbf{q} . The red dashed line is the original estimate of the QE contribution used in Hotta74. The green solid line is the QE contribution determined using our superscaling model. We use these data to extract the longitudinal form factors for nuclear excitations in ^{16}O for the 12.5-20 MeV and the 20-35 MeV regions in excitation energy. **Middle and bottom rows:** The \mathbf{q} dependence of the longitudinal form factor for the 12.5-20 MeV, 20-35 MeV and 35-55 MeV regions in excitation energy.

the QE transverse response function is enhanced at intermediate \mathbf{q} and the longitudinal response function is quenched at low \mathbf{q} . We used the fits in combination with the fits to nuclear excitations to extract $S_L(\mathbf{q})$ for ^{12}C and ^{16}O . In our previous paper we used a very conservative estimate of the uncertainty in the total contribution of the excited states (0.01 plus 15% added in quadrature). In this paper we have updated our fits to the form factors for individual nuclear excitations. We find that the updated total contribution of nuclear excitations to $S_L(\mathbf{q})$ for ^{12}C and ^{16}O is unchanged, but a smaller conservative estimate (0.01 plus 10% added in quadrature) is more appropriate.

The right panel of Fig. 14 shows the various contributions to the extracted $S_L(\mathbf{q})$ for ^{12}C (dotted blue line

with yellow error band). Shown are the QE contribution with only Pauli suppression (dotted-purple), the QE contribution suppressed by both "Pauli Suppression" and the longitudinal quenching factor $F_{quench}^L(\mathbf{q})$ labeled as QE suppressed (Pauli+Quench) (solid-green), and the contribution of nuclear excitations (red dashed line).

The left panel of Fig. 15 shows a comparison of the extracted $S_L(\mathbf{q})$ for ^{12}C (dotted-blue curve with yellow error band) to theoretical calculations. These include the Lovato 2016[3] "First Principle Green's Function Monte Carlo" (GFMC) calculation (solid-purple line), Mihaila[4] 2000 Coupled-Clusters based calculation (AV18+UIX potential, dashed-green), and Cloet 2016[36] RPA calculation (RPA solid-red). Our measurement for ^{12}C are in disagreement with Cloet 2016 RPA,

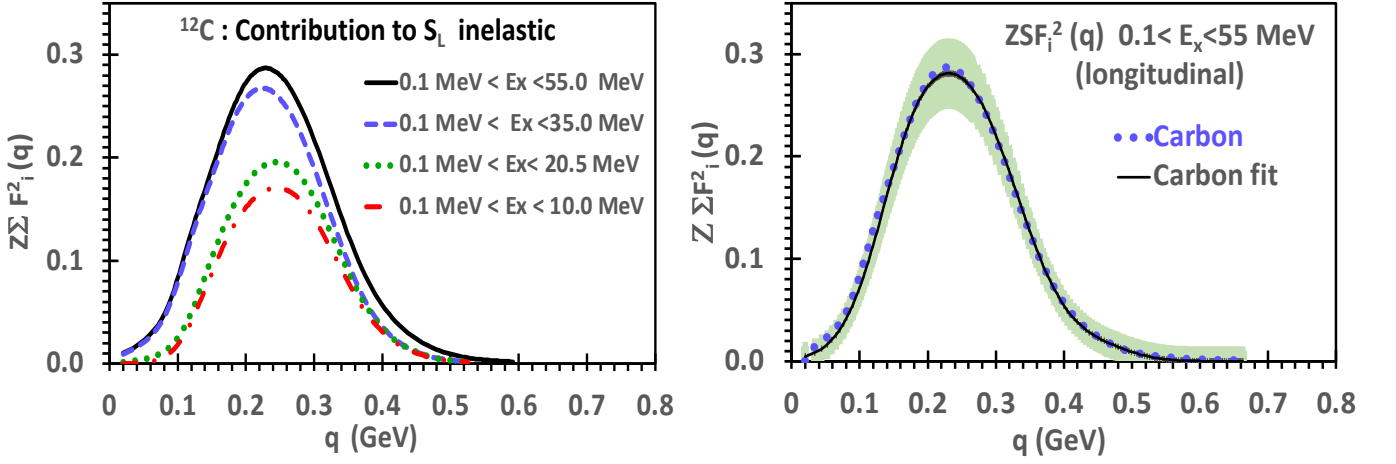


FIG. 12: **Left panel:** The contribution of longitudinal nuclear excitations (between 2 and 55 MeV) to $S_L(\mathbf{q})$ in ^{12}C . **Right panel:** Our fit to the total contributions of all nuclear excitations below 55 MeV to $S_L(\mathbf{q})$ in ^{12}C . The uncertainty (shown as a green band) is 0.01 plus 10% added in quadrature.

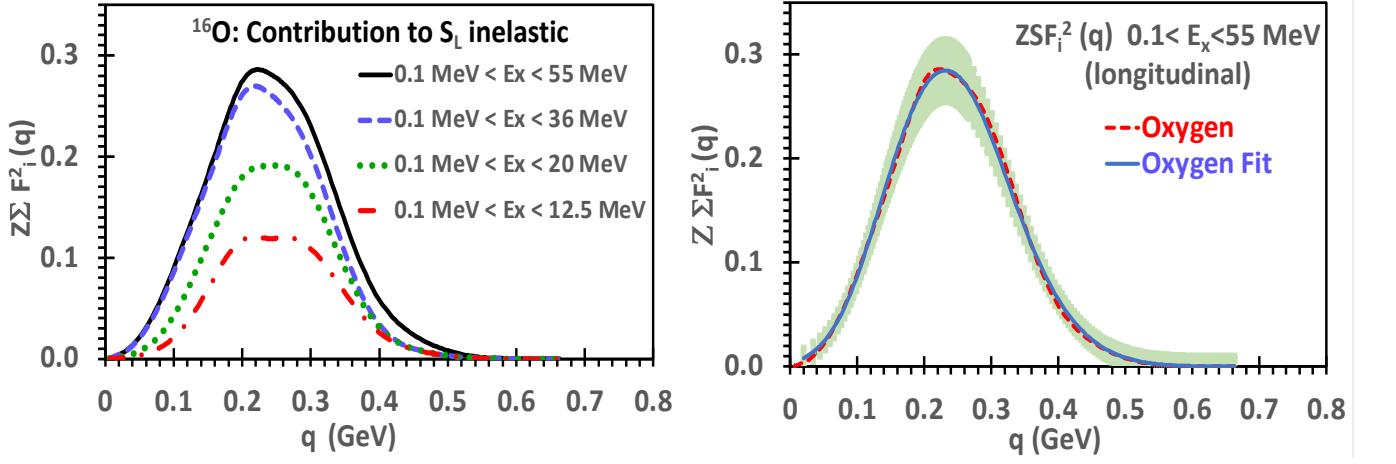


FIG. 13: **Left panel:** The contribution of longitudinal nuclear excitations (between 2 and 55 MeV) to $S_L(\mathbf{q})$ in ^{16}O . **Right panel:** Our fit to the total contributions of all nuclear excitations below 55 MeV to $S_L(\mathbf{q})$ for ^{16}O . The uncertainty (shown as a green band) is 0.01 plus 10% added in quadrature.

and in reasonable agreement with Lovato 2016 except near $\mathbf{q} \approx 0.30$ GeV where the contribution from nuclear excitations is significant.

The right panel of Fig. 15 shows $S_L(\mathbf{q})$ for ^{16}O (dotted-blue with green error band) compared to theoretical calculations. These include the Sobczyk 2020[5] "Coupled-Cluster with Singles-and Doubles (CCSD) NNLO_{sat}" (red-dashed line), and Mihaila 2000[4] Coupled-Cluster calculation with (AV18+UIX potential, dashed green line). The data are in reasonable agreement with Sobczyk 2020.

VIII. SUMMARY

We report on empirical parameterizations of longitudinal and transverse nuclear excitation electromagnetic form factors in ^{12}C and ^{16}O and extract the contribution of nuclear excitations to the Normalized Inelastic Sum Rule $S_L(\mathbf{q})$ as a function momentum transfer \mathbf{q} . We find that the total contribution is significant (0.29 ± 0.030) at $\mathbf{q} = 0.22$ GeV. The total contributions of nuclear excitations in ^{12}C and ^{16}O are consistent with being equal within errors. Since the cross sections for nuclear excitations are significant at low \mathbf{q} , the radiative tails from nuclear excitations should be included in precise calculations of radiative corrections to quasielastic electron scattering at low \mathbf{q} and deep-inelastic electron scattering at

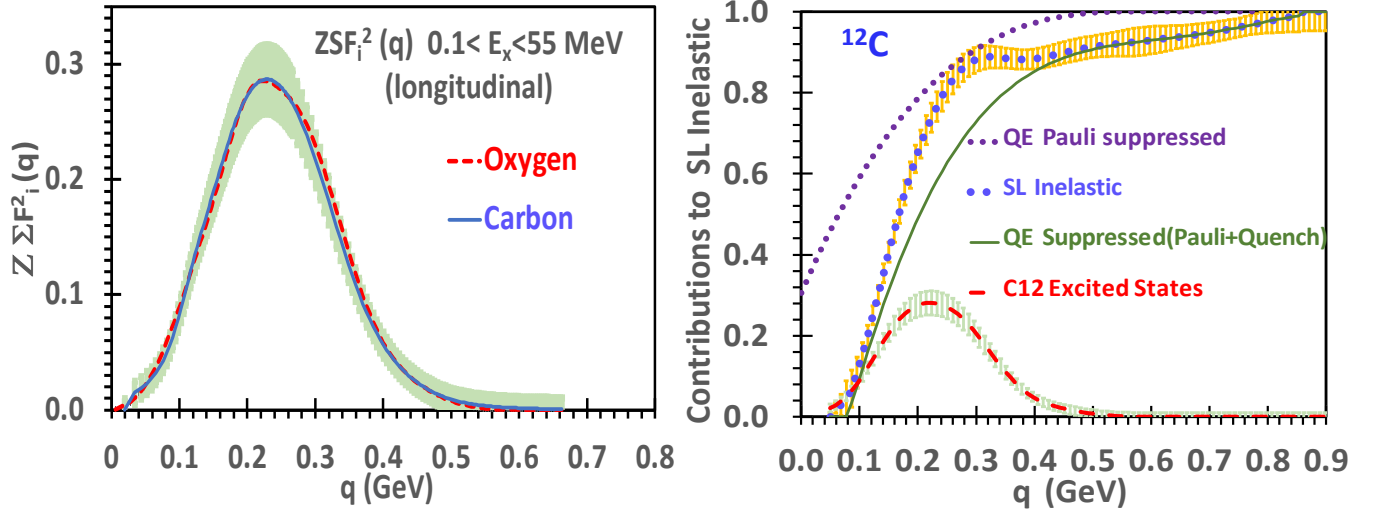


FIG. 14: **Left panel:** A comparison of the contributions of nuclear excitations to $S_L(\mathbf{q})$ in ^{12}C and ^{16}O . The uncertainty (green band) in the total contribution of the excited states is 0.01 plus 10% added in quadrature. **Right panel:** The various contributions[2] to $S_L(\mathbf{q})$ for ^{12}C (dotted blue with yellow error band) including: QE with Pauli suppression only (dotted-purple), QE suppressed by both "Pauli" and "Longitudinal Quenching" (solid-green), and the contribution of nuclear excitations (red-dashed with green error band)

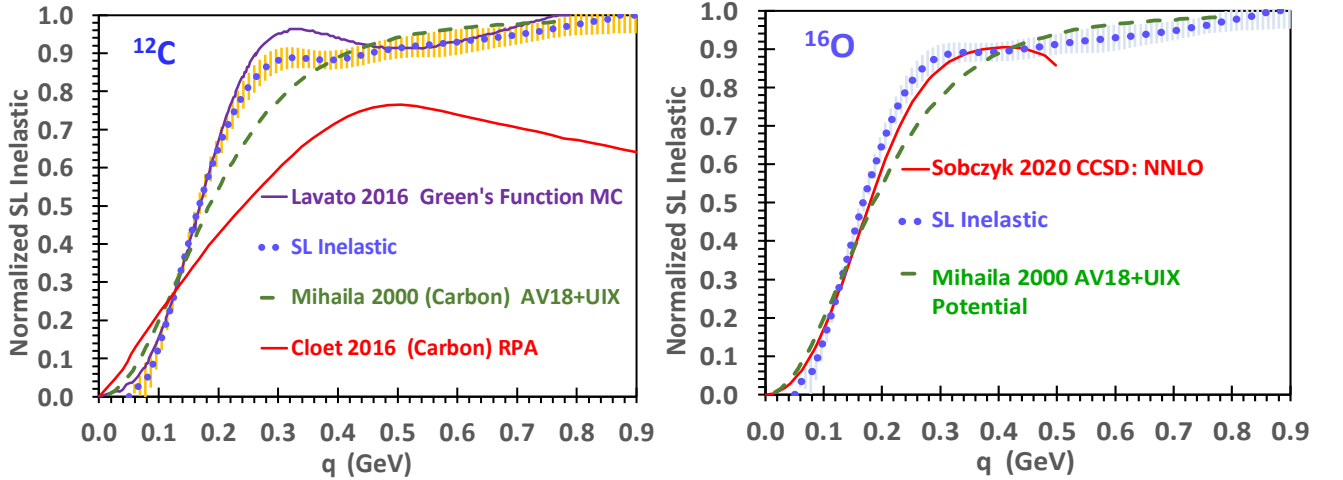


FIG. 15: **Left panel:** $S_L(\mathbf{q})$ for ^{12}C (dotted-blue with yellow error band) compared to theoretical calculations including Lovato 2016 [3] (solid-purple), (Mihaila 2000[4] (dashed-green), and RPA Cloet 2016[36] (solid-red). **Right panel:** $S_L(\mathbf{q})$ for ^{16}O (dotted-black with green error band) compared to theoretical calculations of Sobczyk 2020[5] (red-dashed) and Mihaila 2000 (dotted-dashed).

large ν .

The parameterization also serves as a benchmark in testing theoretical modeling of electron and neutrino scattering cross sections at low energies. Theoretical studies of the excitation of nuclear states in electron and neutrino scattering[6–8] indicate that both are equally significant at low values of \mathbf{q} . Therefore, nuclear excitations should be included in both electron and neutrino MC generators. We note that for excitation energies above proton removal threshold (about 16 MeV in ^{12}C

and 12 MeV in ^{16}O) the decays of nuclear excitations can have a proton in the final state and therefore cannot be distinguished experimentally from QE scattering in low resolution neutrino experiments.

A. Acknowledgments

Research supported in part by the U.S. Department of Energy under University of Rochester grant number DE-

-
- [1] D. Drechsel and M M Giannini 1989 Rep. Prog. Phys. 52 1083 (eq. 7.9); T. de Forest Jr. and J.D. Walecka, *Advances in Physics*, 15:57, 1-109 (1966) (eq. 6.8).
- [2] A. Bodek and M. E. Christy "Extraction of the Coulomb Sum Rule, Transverse Enhancement, and Longitudinal Quenching from an Analysis of all Available e-12C and e-16O Cross Section Data", arXiv:2208.14772 (to be published in *Phys. Rev. C letters* 2022)
- [3] A. Lovato et. al, *Phys. Rev. Lett.* 117, 082501 (2016)
- [4] Bogdan Mihaila and Jochen H. Heisenberg, *Phys. Rev. Lett.* 84 (2000) 1403. 2009.01761 [nucl-th]
- [5] J. E. Sobczyk, B. Acharya, S. Bacca, and G. Hagen *Phys.Rev.C* 102 (2020) 064312.
- [6] V. Pandey, N. Jachowicz, T. Van Cuyck, J. Ryckebusch, and M. Martini, *Phys. Rev. C* 92, 024606 (2015),
- [7] M. Martini, N. Jachowicz, M. Ericson, V. Pandey, T. Van Cuyck, and N. Van Dessel, *Phys. Rev. C* 94, 015501 (2016).
- [8] V. Pandey, N. Jachowicz, M. Martini, R. Gonzalez-Jimenez, J. Ryckebusch, T. Van Cuyck, and N. Van Dessel, *Phys. Rev. C* 94, 054609 (2016).
- [9] H. L. Crannell and T. A. Griffy, *Phys. Rev.* 136, B1580 (1964); H. Crannell, *Phys. Rev.* 148, 1107 (1966).
- [10] Y. Yamaguchi et al., *Phys. Rev. D* 3, 1750 (1971).
- [11] P. Gueye et al., *Eur. Phys. J. A* 56, 126 (2020).
- [12] J.A. Caballero, M. C. Martinez, J. L. Herraiz, J.M. Udias *Physics Letters B* 688. 250 (2010).
- [13] P. Gueye et.al. *Eur. Phys. J. A* 56, 126 (2020); I. Sick, *Nuclear Physics A*218, 509 (1974).
- [14] A. Bodek, S. Avvakumov, R. Bradford, H. Budd, *Eur. Phys. J C*53, 349 (2008).
- [15] T. W. Donnelly and D. Walecka, *Annu. Rev. Nucl. Sci.* 1975.25:329.
- [16] R. Hofstadter, *Annu. Rev. Nucl. Sci.* 1957.7:231-316; *ibid Rev. Modern Physics*, 28, 214 (1956); J. Fregeau and R. Hofstadter, *Phys Rev.* 99.1503 (1955).
- [17] Carbon Elastic and 4.43 MeV and 9.65 MeV form factor measurements: Jerome H. Fregeau, *Phys. Rev.* 104, 225 (1956) (80, 150 MeV); H. L. Crannell and T. A. Grippy, *Phys. Rev.*136, B1580 (1964) (187, 250, and 300 MeV); F. E. Eherenberg et. al., *Phys. Rev.* 113, 666 (1959) (420 MeV); H. Crannell, *Phys. Rev.* 148, 1107 (1966) (600 and 800 MeV); I. Sick and J. McCarthy, *Nucl. Phys. A* 150, 631 (1970) (374.5 and 747.2 MeV, elastic only).
- [18] M. Chernykh et.al. *Phys. Rev. Lett.* 105:022501 (2010),
- [19] P. Strehl and Th. H. Schucan, *Phys. Lett.* 27B, 641 (1968).
- [20] E. A. J. M. Offermann, Ph.D. Thesis, NIKHEF (1988).
- [21] Bates Data (Unpublished) Peter von Neumann-Cosel (private communication).
- [22] Stanford HEPL Data (unpublished) Peter von Neumann-Cosel (private communication)
- [23] H. L.Crannell and T A Gev, *D* 136, B1580 (1964).
- [24] Jerome. H. Fregeau and Robert Hofstadter *Phys. Rev.* 99, 1503 (1955).
- [25] Y. Torizuka et. al., *Phys. Rev. Lett.* 22, 544(1969), M. C. A. Campos et. el. , *Phys. Lett.* B349, 433 (1995).
- [26] J.B. Flanz, R. S. Hicks, R. A. Lindgren, G. A. Peterson, J. Dubach and C. Haxton, *Phys. Rev. Lett.* 43, 1923 (1979).
- [27] N. Nakada, Y. Torizuka and H. Horikawa, *Phys. Rev. Lett.* 27, 795 (1971).
- [28] R. S, Hicks et. al. *Phys. ReV.C*30, 1 (1984).
- [29] C. Maieron, T.W. Donnelly, I. Sick, *Phys.Rev.* C65, 025502, (2002); J.E. Amaro, M.B. Barbaro, J.A. Caballero, T.W. Donnelly, A. Molinari, and I. Sick, *Phys. Rev. C* 71, 015501 (2005); J.E. Amaro, M.B. Barbaro, J.A. Caballero, R. Gonzalez-Jimenez, G.D. Megias, I. Ruiz Simo, *J. Phys. G: Nucl. Part. Phys.* 47, 124001 (2020).
- [30] R. Rosenfelder, *Ann. Phys.* 128, 188 (1980); G. D. Megias, M. V. Ivanov, R. Gonzalez-Jimenez, M. B. Barbaro, J. A. Caballero, T. W. Donnelly, J. M. Udias, *Phys. Rev. D* 89, 093002 (2014); G.D. Megias Vazquez (Tesis Doctoral). Universidad de Sevilla, Sevilla (2017).
- [31] J. Goldemberg and W. C. Barber, *Phys. Rev.* 134, B963 (1964).
- [32] T. de Forest, J. D. Walecka, G. Vanpraet, and W. C. Barber, *Phys. Letters* 16, 311 (1965).
- [33] T. N. Buti et al., *Phys. Rev.*, C33, 755 (1986).
- [34] T. A. Hotta, K. Itoh and T. Saito., *Phys. Rev. Lett.* 33, 790 (1974).
- [35] A. Goldmann and M. Stroetzel, *Z. Phys.* 239, 235 (1970).
- [36] Ian C. Cloet, Wolfgang Bentz, Anthony W. Thomas, *Phys. Rev. Lett.* 116, 032701 (2016).